



NON-ISOTHERMAL RE-START FLOW OF A WAXY CRUDE OIL

Luiz Eduardo Bittencourt Sampaio

Ricardo Sargentini

Luana Valim

Roney Leon Thompson

Universidade Federal Fluminense - Rua Passo da Pátria 156, S^o Domingos, Niterói-RJ, Brasil

luizebs@vm.uff.br,rsargentini@vm.uff.br, lvalim@vm.uff.br, rthompson@mec.uff.br

Abstract. *The flow of waxy crude oils in deep water is an important problem in the oil industry. At this location, the temperature environment can be extremely cold (4 degrees Celsius). The oil generally leaves the reservoir at a high temperature (60 degrees Celsius) when the oil behaves essentially as a Newtonian fluid. However, when there is a break down on the pumping process, the oil is subjected to a cooling process. This cooling makes wax to precipitate, forming crystals that grow, merge with other crystals and transforms the oil into a gel-like material. The gelled oil present some non-Newtonian features and the main one is the presence of a temperature-dependent yield-stress. When there is a shut down for operational reasons, the cooling process is more severe, due to the fact that the fluid is at rest. Farther from the reservoir, the material achieves the environmental temperature and the gelled structure blocks the pipeline. Hence, a non-homogeneous yield stress distribution is obtained. In order to re-start the flow the pressure needed to breakdown the structure of the gelled oil is higher than the steady-state conditions. In this work we numerically solve the flow of a waxy crude oil with temperature-dependent properties in a pipe submitted to different temperature conditions along the tube length. We use a Finite-Volume approach to solve continuity, momentum, and energy equations to account for non-isothermal-non-Newtonian conditions. Different plug-flow profiles are obtained along the pipeline and the pressure conditions for the re-start of the flow is determined. The problem is solved into two stages: the first where the temperature field is solved for zero-velocity conditions, and the second where the re-start flow is solved from that initial conditions.*

Keywords: *waxy crude oils, viscoplasticity, temperature dependency, finite volume*

1. INTRODUCTION

Reservoirs located in deep and ultra-deep water are becoming a more attractive source of oil, since they are located at less explored regions. Generally, the oil that is found in these locations is classified as a waxy crude oil. Waxy crude oil systems are very complex in nature presenting a variety of substances like saturates, aromatics, naphthenes, asphaltenes, and resins. At high temperatures, all these substances are dissolved and the rheological properties of the material are those of a Newtonian fluid. When these waxy crude oils are cooled down, below the so-called *Wax Appearance Temperature* (WAT), which is defined in purely thermodynamic basis, it starts the formation of the first crystals. At this stage, the rheological properties do not change significantly. However, when the oil is subjected to even lower temperature, the *Gelation Temperature* (GT) is achieved and a gel-structure is formed. This gel-like structure is responsible for a considerable change on the rheological material properties and the appearance of an yield stress is a remarkable new character of these kind of materials at low temperatures. Not only the viscosity, but also the yield stress is temperature dependent (Visitiin *et al.*, 2005). The higher is the wax concentration in the oil, higher is the increase in the yield stress value for the same decrease of temperature, below the GT (Oh and Deo, 2009).

The typical temperature in ultra deep water environment is 4°C. The oil inside the reservoir is at a much higher temperature, something around 60°C. Therefore, the heat flux from the flowing material to the environment can be significant and is responsible for cooling the oil inside the duct. This process causes the formation and precipitation of the paraffins that compose the oil. The deposition of such paraffins on the walls of the duct can provoke significant losses in production and understanding the mechanism of formation, precipitation, and deposition of paraffins is essential to control the damage that can occur (Azevedo and Teixeira, 2003). A more unfavorable scenario is achieved when there is a shut down on the pumping process. In this case, the stagnant oil is cooled below the GT causing the formation of the gelled structure in a long portion of the duct, which obstructs the passage of the non-gelled oil near the reservoir.

The re-start problem is a set of strategies that are needed in order return to the normal operational conditions. The new rheological character of the material confers non-Newtonian properties to the waxy crude oil in this gelled state. One of the main new features is the presence of a yield stress, i.e. a viscoplastic property that constitutes a threshold the imposed stress must overcome in order to initiate flow. Therefore, the re-start pressure has to be much higher than the pressure necessary to maintain normal production conditions, since the re-start pressure must cause a stress at the wall that overcomes the yield stress and provoke a breaking up of the gel structure.

The rheological material properties are highly dependent on temperature, therefore the temperature field determines the viscosity and yield stress distribution inside the domain. Since we are interested on the transient response of the

material, starting from a no-flow situation, the initial temperature field is essential for a fair representation of the problem. Besides that, it is incumbent upon us to represent faithfully the temperature dependency of the material properties. As far as the material remains in the Newtonian range, the Arrhenius equation is a suitable choice for representing the viscosity as a function of the temperature. For the non-Newtonian state the Arrhenius equation is not capable to give a reasonable description and a VFTH (Vogel–Fulcher–Tammann–Hesse) model is generally used for a better representation.

The objective of the present work is to numerically simulate the viscoplastic re-start flow problem of a waxy crude oil whose rheological parameters are dependent on temperature. To this end we use the open source code OpenFoam to simulate the balances of mass, momentum, and energy. The material is modeled as a Bingham material. The initial temperature field is obtained from the steady-state solution of the balance of energy when there is no flow.

2. PROBLEM FORMULATION

2.1 Governing equations

The governing equations are given by the mass, momentum, and energy balances of an incompressible non-Newtonian material given, respectively by

$$\nabla \cdot \mathbf{v} = 0 \quad (1)$$

$$\rho \frac{D\mathbf{v}}{Dt} = \nabla \cdot \mathbf{T} \quad (2)$$

$$\rho c_P \frac{DT}{Dt} = -\nabla \cdot \mathbf{q} + \mathbf{T} : \mathbf{D} \quad (3)$$

where \mathbf{v} , \mathbf{T} , and T are the velocity, Cauchy stress, and temperature fields, respectively. \mathbf{D} is the symmetric part of the velocity gradient and \mathbf{q} is the heat flux. The quantity ρc_P represents the heat capacity per unit volume of the material.

2.2 Material constitutive model

The constitutive model for the waxy crude oil considered here is based on a temperature dependent Hershel-Buckley model, but with an viscosity plateau at high shear rates, η_∞ . The temperature dependency of this material should reflect an Arrhenius dependency above the WAT. Besides that, below the WAT, the non-Newtonian features such as yield stress and shear-thinning behavior should come into play and have a non-Arrhenius type of temperature dependency. We use as a non-Arrhenius temperature model, the VFTH equation. Hence, we are assuming that the material has the following constitutive equation

$$\tau = \tau_y(T) + m(T)\dot{\gamma}^n(T) + \eta_\infty(T)\dot{\gamma} \quad (4)$$

where $\tau_y(T)$, $m(T)$, $n(T)$ and $\eta_\infty(T)$ are the yield stress, the consistency index, the power-law index, and the viscosity at high shear rates, respectively. In principle, all these parameters are temperature-dependent. However, In the present work, we do not consider the power-law index to be temperature dependent. For the quantity $\eta_\infty(T)$ an Arrhenius function was assumed, i.e.

$$\eta_\infty(T) = \eta_{\text{ref}} \exp \left[S_\eta \left(\frac{1}{T} - \frac{1}{T_{\text{ref}}} \right) \right] \quad (5)$$

where η_{ref} is a reference viscosity, in this case the viscosity at $T_{\text{ref}} = 60^\circ\text{C}$. For the non-Newtonian parameters we have the following functions with respect to temperature.

$$\tau_y(T) = \bar{\tau}_y \max \left\{ \exp \left[S_{\tau_y} \left(\frac{1}{T} - \frac{1}{\text{WAT}} \right) \right] - 1, 0 \right\} \quad (6)$$

and

$$m(T) = \bar{m} \max \left\{ \exp \left[S_m \left(\frac{1}{T} - \frac{1}{\text{WAT}} \right) \right] - 1, 0 \right\}, \quad (7)$$

where the function $\max\{A, B\}$ returns the maximum value between A and B . We consider a Generalized Newtonian Fluid where the stress tensor, \mathbf{T} , is given by

$$\mathbf{T} = -p\mathbf{1} + \boldsymbol{\tau} = -p\mathbf{1} + 2\eta\mathbf{D} \quad (8)$$

where η is the viscosity given by

$$\eta = \frac{\tau}{\dot{\gamma}}, \quad (9)$$

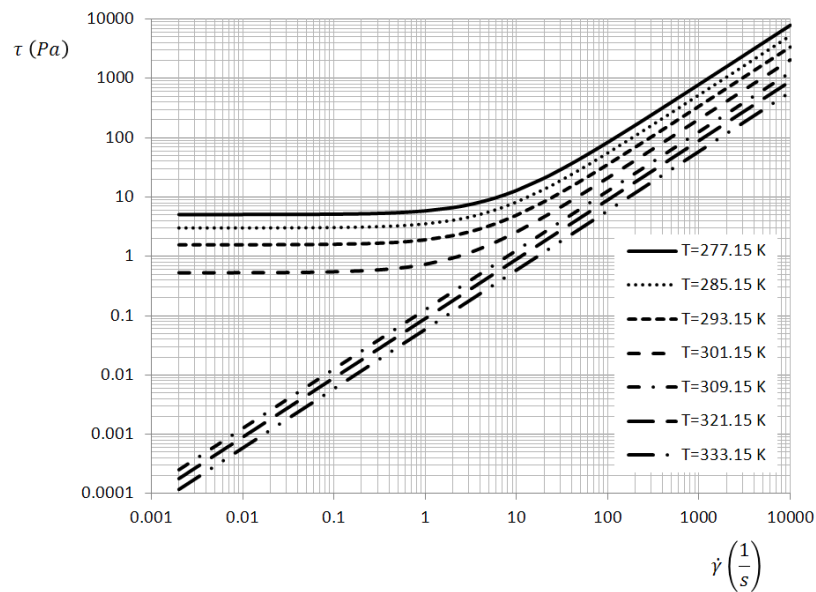


Figure 1. Different flow curves parametrized by temperature.

where τ is given by Eq. (4) and the deformation rate is defined $\dot{\gamma} = \sqrt{0.5\text{tr}(2\mathbf{D})^2}$. Figure 1 shows the qualitative behavior of this family of curves parametrized by temperature.

For the heat flux we assume a simple Fourier material, i.e.

$$\mathbf{q} = -k(T)\nabla T, \quad (10)$$

where k is the thermal conductivity.

2.3 Initial and boundary conditions

The re-start problem is transient in nature. Hence, good estimates for the initial conditions are essential for the representation of the real problem. In this sense, we firstly solve the temperature field, T , corresponding to the shut down conditions, i.e. no flow. In this case, the first law of thermodynamics can be written as

$$\rho c_p \frac{\partial T}{\partial t} = \nabla \cdot k \nabla T, \quad (11)$$

where ρ is the mass density, c_p is the heat capacity, and k is the thermal conductivity of the material. The boundary conditions are meant to reflect, as close as possible, the real problem. The temperature at the entrance of the tube, near the reservoir, is considered uniform and at the reservoir temperature. At the walls, we consider a heat flux proportional to the difference between the wall temperature and the environmental temperature:

$$\mathbf{q}'' = h(T_w - T_\infty), \quad (12)$$

where h is a bulk parameter that depends on the environmental conditions. When there is no flow outside the tube, h is a function of the water thermal conductivity. When there is flow, h plays the role of a film coefficient.

Finally, at the end of the tube we consider a fully developed condition of the form

$$\mathbf{n} \cdot \nabla T = 0. \quad (13)$$

The steady state solution of this problem results in the temperature field that constitutes the initial conditions of the re-start problem. The importance of this first stage of the problem cannot be overemphasized, since the temperature initial distribution determines the initial distribution of the rheological parameters of the material and, hence, are fundamental for the conditions associated to the re-establishment of the flow.

2.4 Dimensionless numbers

A dimensional analysis of the governing equations, boundary conditions, and constitutive equations lead to the following dimensionless numbers

$$N_1 = \frac{hD}{k}, \quad (14)$$

which is equivalent to a Nusselt number.

$$N_2 = \frac{\rho c_p V_c D}{k}, \quad (15)$$

which is equivalent to Peclet number. Where V_c is a characteristic velocity that is related to the pressure drop as $V_c = \sqrt{\frac{2}{\rho} \frac{\Delta p}{L} D}$. The dimensionless quantities associated to the material are given by

$$\tau'_y = \frac{\tau_y(T_c)}{\tau_y(T_c) + m(T_c) \dot{\gamma}_c^n}, \quad (16)$$

where T_c is a characteristic temperature.

2.5 Numerical formulation

The scheme of the problem to be solved is shown in Fig. 2. The oil enters at the tube with the reservoir temperature, $T_R = 60^\circ\text{C}$

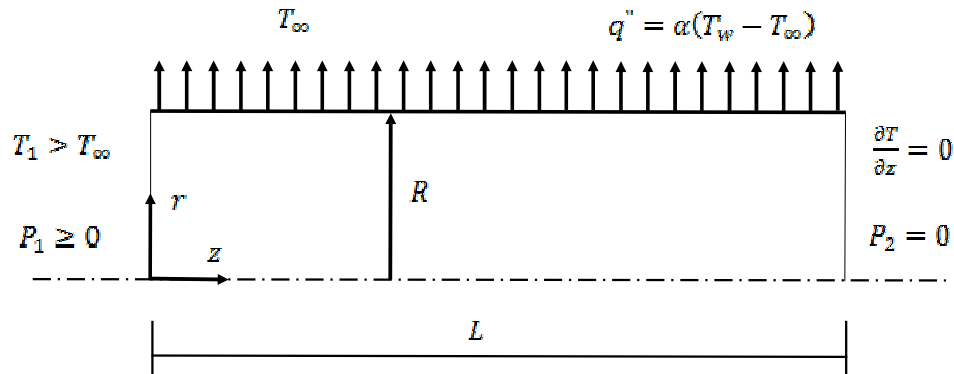


Figure 2. Scheme of the problem.

The computational domain to be considered here spans $R = 0.05\text{m}$ in the radial direction, and $L = 1\text{m}$ in the axial direction. The mesh consists of $80 \times 200 \times 1$ uniform subdivisions in the radial, axial and azimuthal direction, providing the necessary basis for the discretization of the equations.

The mass, momentum, and energy equations were discretized using the Finite Volume Method (FVM) implemented in OpenFOAM (OpenFOAM; Weller *et al.*, 1998). The field values are stored at the control volume centroids. Whenever fluxes or other face quantities are needed, the centroid values are interpolated to the faces centroids, using the most appropriate scheme. Here, a Total Variation Diminishing (TVD) scheme based on Minmod limiter is employed to guarantee a bounded behavior when high frequency oscillations are eminent, yet an accurate discretization for smoother modes.

The discretization of these equations generates three sets of linear systems, corresponding to the mass, momentum, and energy equations, which are solved separately, in a segregated approach. During a time step of the transient evolution, the momentum is solved first, then the pressure is found to correct the mass conservation, and lastly the energy is solved to find the temperature, based on the velocity found in the other two steps. Numerical experiments suggested that the temperature-velocity coupling inside a single time step is far less important than the velocity-pressure coupling. Therefore, an inner loop coupling is performed only for the velocity and pressure fields, using the PISO methodology (Issa, 1986).

3. Results

Starting with a no-flow condition, with a zero pressure gradient and a steady state temperature field given by a pure diffusion equation, an inlet pressure ramp is imposed. This ramp is clipped at a maximum value of $P_1 = 10\text{Pa}$, or, in non-dimensional units, $P_1^* = P_1 D / 4\tau_y L = 357.14$. In Fig. 3(a) the time evolution of this inlet condition is shown as a dimensionless pressure gradient, given by $\nabla P^* = -\nabla P D / 4\tau_y L = P_1 D / 4\tau_y L^2$. The yield stress τ_y is the one corresponding to the cold environment temperature of 4°C , and its value is $\tau_y(4^\circ\text{C}) = 710^{-4}\text{Pa}$. The time is also non-dimensionalized by a characteristic time, according to $t^* = t\sqrt{\tau_y/\rho}/L$. For each time and pressure gradient, the non-dimensional maximum velocity over the whole domain ($U^* = U_{max}/\sqrt{\tau_y/\rho}$) is plotted on the same figure, on the left vertical axes. Figure 3(a) presents the same information, but for a close up around the restart of the flow.

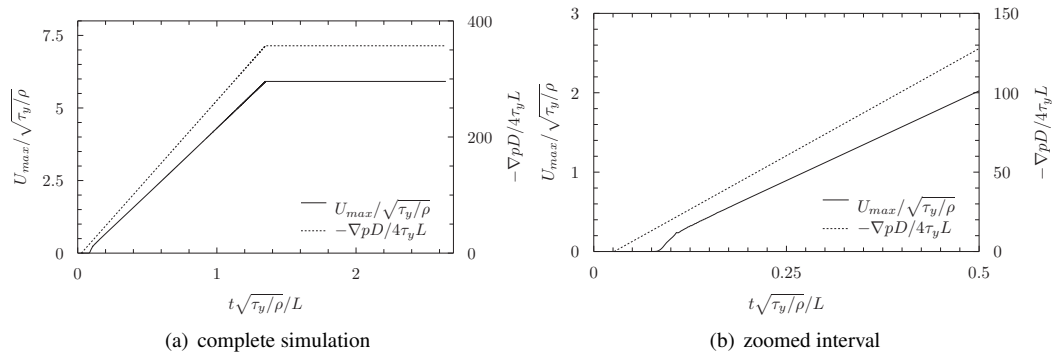


Figure 3. Evolution of the max flow velocity and imposed pressure gradient in time.

One can notice that the maximum velocity linearly follows the pressure gradient trend for most of the simulation. However, near the flow restart corresponding to $t^* = 0.075$, an increase in pressure is not able to move the fluid due to the yield stress for the given temperature. It is interesting to observe that the fluid takes a short time (from $t^* = 0.075$ to $t^* = 0.1$) to go from the no-flow condition to the linear behavior, in which the maximum velocity is proportional to the pressure gradient ramp.

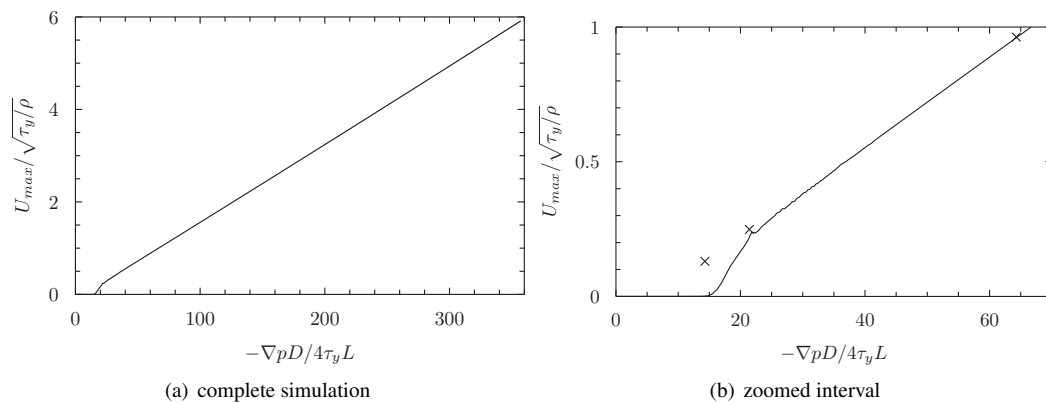


Figure 4. Dependence of the max flow velocity on the imposed pressure gradient.

Figure 4(a) shows the relation between the imposed pressure and the maximum fluid velocity, while Fig. 4(b) shows the same information for a shorter interval. Again, one can see that the linear trend in the fluid movement is not readily established once the pressure reaches a minimum condition for the flow. Instead, it only starts when the pressure gradient is higher than $\nabla P^* = 25$. It remains to be seen whether this is purely related to the dependence of U_{max} on ∇P , or if it has anything to do with a time delay, possibly due to a change in the temperature once the hot fluid invades the duct, affecting greater regions. If the later is actually the case, one could expect to be able to maintain the flow even with a drop in the pressure gradient to $\nabla P^* = 15$, as long as the previous condition consisted of a flowing fluid. Notice that according to the graph in Fig. 4(a), this pressure gradient would not be able to restart the flow, and the ramp would need to keep rising the pressure.

In order to check the causes of this behavior, a further simulation was ran (Fig. 5), in which the pressure was changed to gradually smaller values ($P_1 = 1.8, 0.6, 0.4$) in steps, beginning from a established flow condition – the same found in the end of the ramp simulation. For each of these pressure steps, enough time was simulated in order to allow reaching steady state before changing to the next pressure value. This can be verified by looking at the quick exponential decay of velocity after each change in pressure, in the same Fig. 5.

The dependence of U_{max} on ∇P for this stepped pressure simulation is plotted with cross symbols (“×”) in Fig. 4(b), in order to be readily compared to the former restart ramp simulation. It is clear that during this latter simulation there is a fluid flow, even for the lower pressure values, the same of which could not restart the flow in the ramp following a no-flow initial condition. The reason for this can be easily understood by observing that, for the new initial flow condition, the high temperatures of the inlet region have stronger influence in the domain interior. Thus, the temperatures inside the tube tend to be higher, with a lower yield stress. Also of interest is the observation that this stepwise decrease in pressure promoted a linear decrease trend in the maximum velocity. This suggests that a possible strategy to the restart problem would be to impose a higher pressure in the beginning to guarantee a faster hot fluid entrance in the tube, followed by a

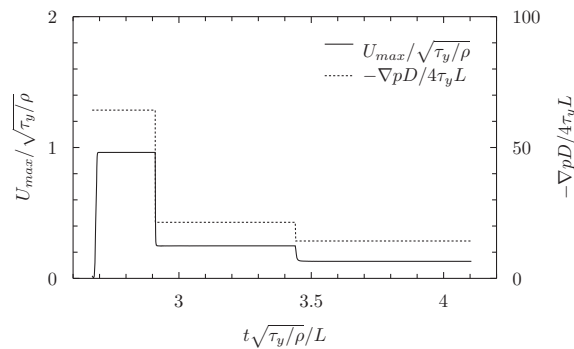


Figure 5. Evolution of the max flow velocity and imposed pressure gradient in time for the piecewise stepped pressure evolution.

lower pressure just enough to maintain the flow, taking advantage of the smaller yield stresses involved due to the higher temperatures.

Figure 6 presents the profiles of temperature and yield stresses for different axial positions along the pipe, for the last step of pressure, in steady state. The dimensionless temperature is given by $\theta = (T - T_\infty)/(T_1 - T_\infty)$, while the dimensionless yield stress is given by $\tau_y^* = \tau_y/\tau_{y_c}$. Here, $\tau_y = \tau_y(T)$ is the yield stress for the local temperature, while τ_{y_c} is the yield stress for the cold temperature of reference, $T_\infty = 4^\circ\text{C}$.

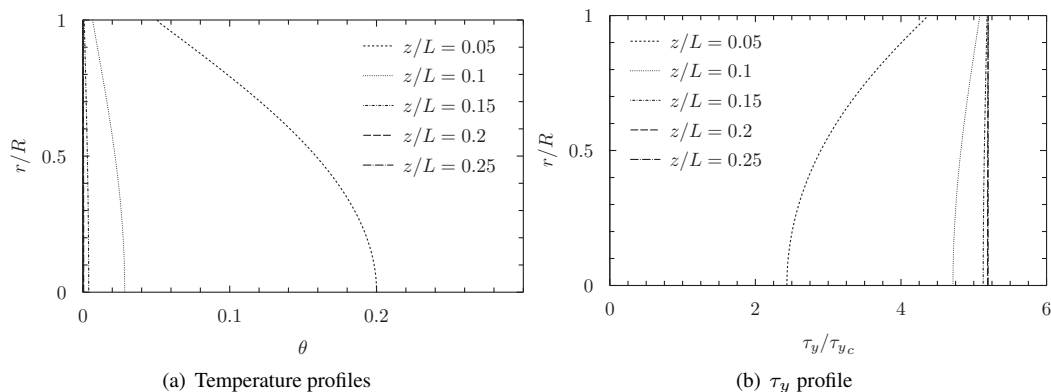


Figure 6. Profiles of temperature and corresponding yielding stress.

One can see that in both Figs. 6(a) and 6(b) the profiles are already well developed and totally dominated by the environment temperature (T_∞ , with $\theta = 0$) at a quarter of the total length, or at five radii ($5R$). At the inlet and its vicinity, the temperatures are higher and closer to the hot oil ($\theta = 1$), and consequently the yield stresses are reduced.

Figure 7 compares two sets of profiles for the same pressure gradient ($\nabla P^* = 64.28$). However, one of these sets (Fig. 7(a)) is taken during the transient increasing pressure ramp (starting from a no-flow condition), while the other (Fig. 7(b)) is taken in the steady state reached with a fixed pressure after the restart. No appreciable difference is noted between these two situations, meaning the ramp is slow enough to allow a quasi steady state at each pressure value, at least for this high pressure value.

The next two figures (Fig. 8(a) and 8(b)) present the profiles at the same locations for the other two steady states conditions, reached by the application of the decreasing stepwise pressure, following a previously established flow condition. One can observe the onset of the plug flow, which is bigger for the smaller pressure gradient, as it competes in magnitude with the yield stress.

4. FINAL REMARKS

We developed a procedure to solve the non-isothermal flow of waxy crude oil in pipeline in the re-start conditions, i.e. when there is a interruption of the normal conditions and the oil is subjected to low temperature environment conditions. In this case, the oil exhibit non-Newtonian features with rheological parameters that are dependent on temperature. The transient solution is obtained via a Finite Volume formulation implemented in OpenFoam. The preliminary results obtained were very satisfactory, qualitatively with the expected trends.

A ramp in the pressure drop provided information about the minimum value necessary to overcome the resistance imposed by the yield stress. There is a clear value, below which the material does not move.

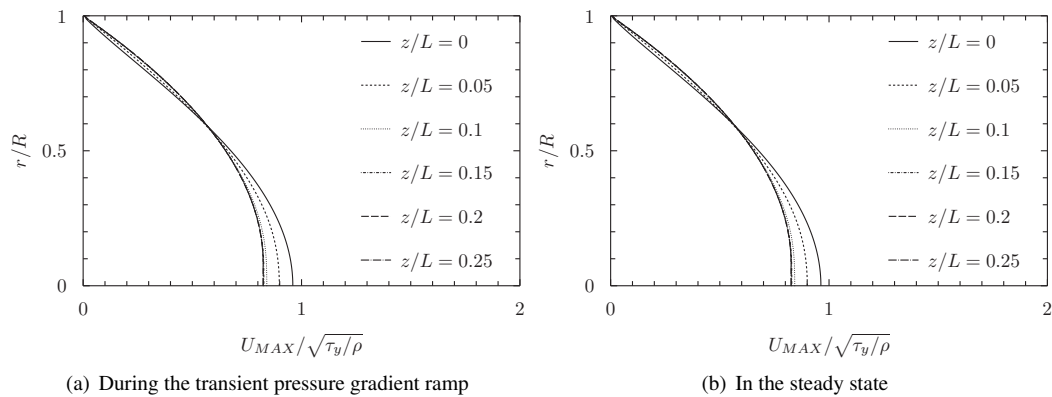
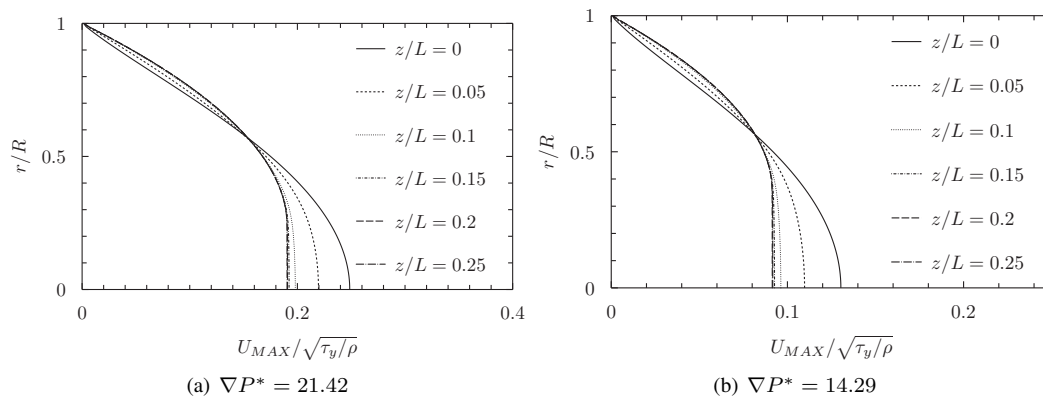
Figure 7. Velocity profiles for $\nabla P^* = 64.28$.

Figure 8. Velocity profiles for steady state solution.

The velocity profile is more parabolic at the positions of higher temperature, where the material is predominantly Newtonian, and present a plug flow at regions where the temperature is lower, and the fluid acquires more viscoplastic features.

5. REFERENCES

- Azevedo, L.F.A. and Teixeira, A.M., 2003. "A critical review of the modeling of wax deposition mechanism". *Petr. Sci. Tech.*, Vol. 21, pp. 393–408.
- Issa, R.I., 1986. "Solution of the implicitly discretised fluid flow equations by operator-splitting". *Journal of Computational Physics*, Vol. 62, pp. 40–65. doi:10.1016/0021-9991(86)90099-9.
- Oh, K. and Deo, M., 2009. "Characteristics of wax gel formation in the presence of asphaltenes". *Energy & Fuels*, Vol. 23, pp. 1289–1293.
- OpenFOAM, 2013. "Openfoam manual". <http://www.openfoam.org/>.
- Visitin, R.F.G., Lapasin, R., Vignati, E., D'Antona, P. and Lockhart, T.P., 2005. "Rheological behavior and structural interpretation of waxy crude oil gels". *Langmuir*, Vol. 21, pp. 6240–6249.
- Weller, H.G., Tabor, G., Jasak, H. and Fureby, C., 1998. "A tensorial approach to computational continuum mechanics using object-oriented techniques". *Computers in physics*, Vol. 12, pp. 620–631.

6. RESPONSIBILITY NOTICE

The authors are the only responsible for the printed material included in this paper.